Published in final edited form as:
Methods Cell Biol. 2013 ; 118: 195–216. doi:10.1016/B978-0-12-417164-0.00012-4.

Photobleaching Methods to Study Golgi Complex Dynamics in Living Cells

Erik Lee Snapp
Department of Anatomy and Structural Biology, Albert Einstein College of Medicine, New York, USA

Abstract

The Golgi complex (GC) is a highly dynamic organelle that constantly receives and exports proteins and lipids from both the endoplasmic reticulum and the plasma membrane. While protein trafficking can be monitored with traditional biochemical methods, these approaches average the behaviors of millions of cells, provide modest temporal information and no spatial information. Photobleaching methods enable investigators to monitor protein trafficking in single cells or even single GC stacks with subsecond precision. Furthermore, photobleaching can be exploited to monitor the behaviors of resident GC proteins to provide insight into mechanisms of retention and trafficking. In this chapter, general photobleaching approaches with laser scanning confocal microscopes are described. Importantly, the problems associated with many fluorescent proteins (FPs) and their uses in the secretory pathway are discussed and appropriate choices are suggested. For example, Enhanced Green Fluorescent Protein (EGFP) and most red FPs are extremely problematic. Finally, options for data analyses are described.

INTRODUCTION AND RATIONALE

George Palade's Nobel prize-winning discovery that secretory proteins move between membranous cellular compartments raised several interesting questions. Do secretory proteins move from the endoplasmic reticulum (ER) to the Golgi complex (GC) to the plasma membrane or extracellular milieu in a unidirectional manner? Are the proteins compartmentalized into a single structure that matures into different types of compartments or do proteins move between distinct compartments? Within the compartments, are the proteins part of an immobilized matrix or do the proteins freely diffuse within a compartment. How and where are proteins sorted for different fates and destinations (such as the lysosome vs. the plasma membrane)? How fast do different proteins move through the secretory pathway? How are proteins retained or enriched in different compartments of the secretory pathway? All of these questions have been addressed to varying degrees with classical imaging techniques including immunogold transmission electron microscopy, immunofluorescence microscopy, biochemistry, and genetics.

However, the techniques are generally static (only capturing a single time point). Biochemistry experiments average the behaviors of millions of cells, which may be in different stages of the cell cycle, apoptotic, damaged, or differentiating. Fixed cell imaging experiments also do not illuminate how molecules behave within a cell, just that the molecules have a particular distribution.

Live cell imaging with dye-labeled proteins or organelle dyes provided new insights into the dynamics of cellular compartments. Yet, the cloning of green fluorescent protein (GFP) was the technological advance that now enabled investigation of the dynamics of proteins in cells, especially proteins in the early secretory pathway, as one cannot microinject dye-labeled proteins into the extremely small ER or GC. GFP-labeled proteins and the compartments they label can be visualized readily in live cell fluorescence microscope setups. Still, these proteins offer no insight into their organization or mobility within a compartment. The compartment is simply green.

Combining GFP-labeled proteins with laser scanning confocal microscopy opened up a new frontier and now with the application of photobleaching techniques, one could directly investigate the mobility and organization of proteins in cells (Lippincott-Schwartz, Snapp, & Kenworthy, 2001). Better yet, the availability of other colors of fluorescent proteins (FPs) meant that multiple proteins can be monitored simultaneously, not just in solution, but in the actual native cellular environment. Photobleaching technology is possible on confocal microscopes available at most universities. In this chapter, a guide to successfully perform and interpret photobleaching experiments is described.

12.1 MATERIALS

1. Imaging medium: Phenol red free medium (such as RPMI or DMEM), 10% fetal bovine serum, 2 mM glutamine, 25 mM HEPES, pH 7.4. Other cell types may require different media. Note that phenol red is a chromophore that will absorb light and thus decrease the effective illumination of a sample. More importantly, phenol red can contribute to background and can even mark lysosomes in cells illuminated with near UV light. The important things are to keep cells supplied with energy (from media), growth factors (serum), and to avoid the negative effect of phenol red dye on fluorescence imaging. Media must not contain this dye.
2. Formaldehyde/PBS (phosphate-buffered saline) containing either 3.7% freshly diluted formaldehyde (from 37% stock) or 4% fresh paraformaldehyde.
3. Transfected eukaryotic cells expressing desired GFP chimeric protein or cells with plasmid plus transfection reagent or virus for expressing protein of interest.
4. Cell culture medium (i.e., DMEM with serum) for cell culturing and transfection.
5. Inverted Confocal Laser Scanning Microscope equipped with a filter set for GFP and a 488-nm excitation laser that is at least 10 mW and preferably 25 mW or more powerful laser and an acousto-optical transmission filter (AOTF). Suitable commonly available Zeiss LSM 510 or 710 with the physiology software package, Leica SP2, 5, and 7, Olympus FV1000 and FV1200 (Olympus Corporation of the Americas, Center Valley, PA), Nikon A1 (Nikon Instruments, Inc., Melville, NY) or a microscope with a pointþscanning laser regulated by an AOTF. For example, some of the newer spinning disk confocal microscopes (UltraVIEW) have photobleaching laser modules (i.e., Perkin Elmer, Waltham, MA).

6. Imaging chamber (either a Nunc Lab-Tek chambered coverglass (Fig. 12.1) or MatTek dish (Ashland, MA)).
7. Immersion media (i.e., oil for oil microscope objectives).
8. Stage heater or environmental chamber (for cells that grow at temperatures above 28 °C).
9. A computer system capable of processing large image files (a 100+-GB hard drive, and at 2-GB RAM) equipped with image processing software (i.e., NIH Image, Matlab (TM), Volocity (TM), or Metamorph (TM)).

12.2 METHODS

12.2.1 Choice of FPs for studies of the secretory pathway

Not all FPs are created equal. In fact, many FPs have very specific uses and are not interchangeable. While brightness, photostability, and folding time are all important properties for an FP, there are X key features that are often not considered. The FP must be suitable for the particular cellular environment. All natural FPs (such as GFP and DsRed) and most evolved FPs (i.e., mCherry) are from the cytoplasm of various eukaryotes and bacteria. This becomes a concern when putting an FP inside the secretory pathway. First, FPs often contain cysteines. In the oxidizing environment of the secretory pathway, the FPs can form interchain disulfide bonds that result in dark misfolded proteins (Aronson, Costantini, & Snapp, 2011; Jain, Joyce, Molinete, Halban, & Gorr, 2001). While a fluorescent signal may be present, 50% or more of the FP pool can be misfolded and dark. This dark pool will decrease overall fluorescent signal and will complicate the interpretation of biochemical assays using the secretory FP, as only part of the pool of fusion protein may actually be functional. Second, many FPs contain consensus sequences (N-X-S/T, where X is any amino acid except proline) for N-linked sugar additions. These sugars increase an FP's size and can influence its diffusive behavior (Costantini, Subach, Jaureguiberry-Bravo, Verkhusha, & Snapp, 2013) and cause a fusion protein to interact with the lectin chaperones calnexin and calreticulin. Third, FPs have a characteristic pK_a or pH at which the fluorescence intensity of the FP decreases by half and eventually becomes dark as the pH decreases further. In the neutral pH of the cytoplasm or the ER, this is not an issue. However, the successive compartments of the GC are increasingly more acidic, such that higher pK_a FPs (including EGFP 6.0, EYFP 6.9, Venus 6.0, and mKate 6.0; Shaner, Patterson, & Davidson, 2007) may be quite dim in the pH 6.0 trans GC (Paroutis, Touret, & Grinstein, 2004). Finally, regardless of whether the FP is in the lumen of the GC or associates with the GC surface in the cytoplasm, it is critical that the FP be truly monomeric. Many FPs are not and FPs that are labeled as monomeric may not be (i.e., TagRFP; Costantini, Fossati, Francolini, & Snapp, 2012). The ability of FPs to oligomerize can affect everything from causing false-positive signals in Förster Resonance Energy Transfer (FRET) experiments (Zacharias, Violin, Newton, & Tsien, 2002) to gross distortion of secre-tory organelles when FPs on apposing membranes interact (Snapp et al., 2003). In some cases, it is not even a matter of simple oligomerization. Some red FPs are relatively monomeric, but have a tendency to cluster or aggregate at high concentrations. This is particularly problematic when FPs are attached to membrane or membrane-associated

proteins. By confining FPs to the two-dimensional surface of a membrane, the effective concentration substantially increases. Even weak dimerizing activity that is not problematic for soluble cytoplasmic proteins becomes a serious issue on a membrane surface.

Standard GC fluorescent reporters, such as the Galactosyl Transferase (GalT) FP construct, can adversely affect GC size and organization if a sticky or oligomerizing FP is incorporated (Fig. 12.2). Only an environmentally neutral FP should be used for a fusion protein, in general, and in particular for a GC membrane protein reporter. As with any FP reporter, it is important that the investigator establishes that the reporter does not alter the structure (unless is an experimental goal) or function of the GC.

To date, expression of red FPs typically distorts the GC at all but the lowest levels of expression. EGFP and related FPs do not distort the GC, but a large pool typically misfolds in the oxidizing lumen of the secretory pathway. The best behaved FPs we have identified are superfolder GFP (sfGFP) and its derivatives (Aronson et al., 2011; Pedelacq, Cabantous, Tran, Terwilliger, & Waldo, 2006). A blue FP suitable for the secretory pathway has been described (Costantini et al., 2013) and can be used in conjunction with sfGFP without significant crosstalk for most microscope filter sets. FPs with cysteines or N-linked glycosylation sites can be used on the cytoplasmic face of the GC, as long as the FPs are robustly monomeric.

Even with an optimal FP, the investigator is cautioned against selecting high expresser cells for imaging. Many cellular proteins are expressed at modest to very low (hundreds to thousands of molecules per cell). With a bright FP, some constructs, if expressed at near endogenous levels, may still not be easily detected. Within the tightly packed GC, this is often less of a concern. When a small number of molecules are concentrated in a tight space, the fluorescent signal can be excellent.

12.2.2 Cell culture and transfection

Before performing a photobleaching protocol, the investigator must ensure that there is sufficient fluorescent signal in the expressing cell relative to background noise after photobleaching. Thus, a sufficient number of cells expressing the fluorescent reporter must be ensured.

To image adherent cells, they are typically grown on coverglass discs or in multi-well chambers (Nunc Lab-Tek, #1 coverglass, especially for use with samples thicker than one layer of cells). We prefer the latter because cells retain their full three-dimensional shapes, while coverslips are often pressed against slides and the cells are squished. Plate the cells on the sterile coverglass in media of choice at least 16 h in advance. The next day, prewarm freshly prepared imaging media (to 37 °C for mammalian cells). Aspirate the growth media and replace with imaging media covering the cells generously, that is, 400 ml of imaging media per well in an eight-well Lab-Tek chamber.

To image suspension cells, the cells can be adhered to a coverglass that has been pretreated with concentrated poly-L-lysine. To successfully stick the cells to poly-L-lysine, the cells must be in a medium free of proteins, that is, 1 PBS. Any negatively charged material can

bind to the poly-L-lysine and compete with the cells for binding. The serum in cell media will completely prevent adherence of cells to poly-L-lysine.

First, add concentrated poly-L-lysine (P8920 from Sigma-Aldrich, St. Louis, MO) to coverglass and incubate for 5 min. Remove poly-L-lysine and save it, as it can be reused multiple times. Wash the coverslip 2 × in dH_2O and allow to air dry. This can be done sterilely in a tissue culture hood if the cells are to be imaged for more than a few hours. Spin suspension cells at low centrifuge speed to gently pellet, resuspend in PBS, spin, and resuspend again in a low volume of PBS. Add to and cover the coverglass chamber, incubate 5 min at RT, wash 2 × gently with PBS, and then add imaging media.

If the cells are not stably expressing an FP construct, then the construct should be transfected at least 8–16 h in advance using cationic lipids (i.e., FuGENE6 (Roche, Indianapolis, IN) or LipofectAMINE 2000 (Invitrogen, Carlsbad, CA)) or a viral vector. Alternatively, electroporation can achieve high transfection efficiency. The optimal level of expression and timing of imaging should be determined empirically for each construct, cell type, and condition.

Transfection protocols will vary depending on the volume and cell type. Our lab typically uses Lipofectamine 2000 with good results for several tissue culture cell lines. Whichever transfection method is selected, the investigator needs several usable cells for each experiment. Note that for microscopy experiments, high transfection efficiency (70–100%) is not necessary and is often undesirable. Good images are often achieved at lower efficiencies so that individual cells can be readily distinguished. 10–40% efficiency is a good range for imaging single cells. Cells expressing low to modest levels of FPs are preferable for imaging. While high expressing cells are easier to image, the high expression levels may perturb GC structure and/or function. Note that stably expressing cells usually express a construct at comparably low levels of protein and this is also desirable. Higher expression levels can lead to GC structure artifacts, protein aggregation or titrate fusion protein cofactors.

12.2.2.1 Preparing the imaging chamber

1. When using an inverted microscope, adherent cells can be plated on Lab-Tek chambers (Nalgene, Naperville, IL). These chambers consist of wells with a cover glass bottom, which permits the use of high numerical aperture oil objectives for viewing. Prior to placing the cells on the microscope stage, the wells are filled to the rim with imaging media. This ensures that cells have sufficient nutrients during the imaging session. For experiments that will last longer than an hour, the top cover of the chamber should be sealed onto the chamber using petroleum jelly or silicon grease. These steps prevent both rapid evaporation of the media above the cells and decrease the alkalinization of the media by preventing room air from entering the chamber. Suspension cells can be grown in suspension and then adhered to coverslips or Lab-Tek chambers by precoating the chamber or clean coverslip with a concentrated (5–10 mg/ml in PBS) solution of poly-L-lysine (Sigma-Aldrich, St. Louis, MO). Incubate for 5 min. Wash twice with dH_2O. Suspension cells first must be washed three times in PBS, before adhering to the

poly-L-lysine-coated surface. Incubate the cells on the surface for 2–5 min. Remove the nonadhering cells with PBS (wash twice). Then cover the cells in imaging medium.

2. Maintain cells at physiological temperature on the microscope stage using a stage heater, such as the Model ASI 400 Air Stream Stage Incubator (Nevtek, Burnsville, VA), an environmental chamber or even a thermal collar objective heater (Bioptechs, Butler, PA). A temperature probe, such as a Thermolyne Pyrometer (Carl Parmer, Vernon Hills, IL), can be used to confirm maintenance of the temperature at the chamber.

12.2.3 Preparing the imaging system

Set up the confocal laser scanning microscope and its associated hardware. The investigator should be familiar with the basic operation of the confocal microscope. It is worth understanding both the concept and the operation of a pinhole, scan speed, zoom, detector gain, laser power, photobleach, and how the microscope collects a time series. The protocols in this chapter are guidelines and conditions will differ depending on laser power, scan speed, detector sensitivity, and sample properties. Understanding microscope principles will free the investigator to adapt protocols to his/her microscope.

12.2.3.1 Defining the capabilities of your confocal microscope—Before planning photobleaching experiments, it is vital to evaluate the status and abilities of the laser scanning confocal microscope. First, it is important to determine whether the microscope can deliver sufficient laser power for the FP of choice, that is, a 488-nm laser to photobleach sfGFP. This typically must be determined empirically. Even if a microscope has photobleaching capabilities, the laser may be too weak, may be out of alignment or may need to be replaced. Standard imaging experiments are often not a problem for a weak laser, as one can simply increase laser power to the sample. Photobleaching experiments demand substantial laser power that often starts with a laser of 10 mW power or higher. Lower powers can be used, but will be useful often only for slowly diffusing proteins or for FLIP experiments.

How can one assess the microscope's capabilities? An appropriate sample slide is needed with cells expressing the FP of choice. To avoid complexities of FP movements, the sample must be fixed. Wash the coverslip or Lab-Tek chamber once with 1 × PBS, aspirate, and add freshly prepared 3.7% formaldehyde in 1 × PBS and in cubate in a dark drawer at RT for 15 min. Remove the formaldehyde and store in a chemical hazard container and add back 1 PBS to the fixed cells.

Start up the confocal microscope according to protocol. Prewarm lasers for at least 5 min and then prepare to image. Select a high numerical aperture (NA) objective to maximize light collection. Excellent results can be obtained with a 60–63 × NA 1.4 objective. 40 × also works well and 100 ×, too. The 100 × objective typically causes samples to appear dimmer due to the relationship between magnification and brightness. For most imaging needs, the 100 × objective is rarely optimal.

Apply the appropriate medium to the objective, that is, oil, water, glycerol or other media and position the sample. Use the oculars to find and center a cell of interest. Switch to laser scanning mode and image the cell with low laser power, the highest speed that still maintains a sufficiently bright image (i.e., 15% or more of the intensity range of the image scale, 50 for an 8-bit image or 600 for a 12-bit image). Avoid saturated pixels, as these are not suitable for quantitative imaging. Saturated pixels are literally intensity values higher than the detection scale and represent lost information. The pinhole should be open to maximize the sample signal. Note that the pinhole is positioned at the end of the light path, in front of the detector. Therefore, the pinhole has no effect on photobleaching efficiency. The key for most photobleaching experiments is quantitative signal, not necessarily attractive images.

Most photobleaching modules have a specific software program or macro. Open the program or macro and apply settings to define a photobleach region. Acquire a prebleach image for comparison. For maximum speed, use a horizontal box or region of interest (ROI). Set the photobleaching parameters for one iteration of photo-bleaching intensity laser power and attempt to photobleach the region of interest. If the region bleaches, then the conditions can be minimized until bleaching conditions achieve 70–90% bleach depth (completion).

If little or no bleaching is detected, modify parameters to increase bleaching. These conditions include the scan speed of the bleaching laser (slower bleaches more strongly), the zoom of the cell (higher zoom increases sample bleaching), number of scans, and activating other laser lines (i.e., sfGFP can be bleached by a 488-nm line, but also by the 514-, 456-, and 478-nm lines typically found on argon lasers. Similarly, mCherry photobleaches poorly with a 1-mW 543-nm laser, but has sufficient absorbance spectrum that even a 488-nm laser can help photobleach a sample.

The optimal bleaching conditions will depend on the type of microscope and its components. For a 63 × NA 1.4 objective on a Zeiss 510 with 40-mW 488-/514-nm Argon or 25-mW argon laser are 45–60% power with 100% transmission. For acquisition of recovery time points, use the same level of power with only 0.1–1.0% transmission (if possible), as regulated by the AOTF. For quantitative Fluorescence Recovery after Photobleaching (FRAP), the whole cell is usually scanned at scan speed 8–10 (0.798–3 s per 512 512 frame) with either two line averaging or no line averaging. For a Zeiss Duoscan with a 100-mW 489-nm laser, sfGFP is bleached using a 63 × NA 1.4 objective with one to three iterations at zoom 1, photobleaching laser scan speed of 6 with 100% transmission through an 80/20 beam splitter, with only 20% of laser power dedicated to the photobleaching scanner. Imaging is performed at 5 frames per second (fps) or faster with 0.5–1.5% transmission, and no frame averaging. For faster imaging, the cell of interest is often centered and a strip of only 100–200 pixels *Y*-axis of the normally 512 × 512 field is scanned.

If photobleaching cannot be performed rapidly or at all, it is often worth a visit from a service technician to align the laser (a common cause of low power) or the laser may need to be replaced. If everything is working to specifications, then the instrument may not be suitable for photobleaching experiments.

12.2.4 FRAP protocol

To perform data analysis of an FRAP experiment (Fig. 12.3), the user must collect at least one prebleach image of the cell, a series of postbleach images of the whole cell that extends from an immediate postbleach image to several images after the bleach ROI fluorescence intensity reaches a plateau, and a table of fluorescence intensity values including the photobleach ROI, the whole cell ROI, and a background ROI. The investigator also needs to know the corresponding time for each image and the image pixel size in microns. For the Zeiss 510 microscope, the physiology software package contains several windows that permit the user to determine the number of images to collect, laser intensities for bleaching and imaging, number of bleach iterations, how many images to collect before bleaching, and drawing of the photobleach ROI. Other microscopes may or may not contain their own software package or may require writing macros for the photobleach time series.

A quick note on software packages. It is important for the investigator to appreciate that not all software packages necessarily do the same thing. That is, some definitions of photobleaching experiments differ between companies. On the Leica SP2, for example, the FLIP wizard will only collect a prebleach image and an image at the end of the FLIP experiment. This protocol is not a true FLIP experiment and is of debatable utility. Some microscope company software packages also include analysis software. This author has tried three of them and, to date, has not found a diffusion analysis program that correctly calculates the diffusion coefficient (*D* value) for proteins of known mobilities. The take home message is not that it is impossible to calculate D values, but that investigators serious about quantitative microscopy should test any new system with standards with well-established properties. For example, cytoplasmic GFP diffuses at ~23 mm^2/s (Lajoie& Snapp, 2010; Swaminathan, Hoang, & Verkman, 1997) and the membrane protein Vesicular Stomatitis Virus G protein fused to GFP (VSV G-GFP) diffuses at 0.45 $\mu m^2/s$ in the ER membrane (Nehls et al., 2000). GalT GFP, which uses a luminal GFP to replace the enzymatic domain of this GC integral membrane protein, diffuses at 0.3–0.5 $\mu m^2/s$ (Cole et al., 1996):

1. Collect multiple prebleach images to establish the prebleach fluorescence intensity and to confirm that the prebleach fluorescence intensities of the cell and the bleach ROI do not fluctuate significantly.
2. Photobleach the ROI with intense laser illumination. Continue to image the whole cell at low laser illumination (the same conditions as the prebleach images), until the recovery process has reached a steady state. These conditions must be determined quantitatively, as the human eye is incapable of distinguishing small differences in intensities. Typically, a 1- to 4-μm wide bleach ROI strip will recover within 30–120 s for most freely mobile soluble lumenal proteins and within 3–5 min for membrane proteins in the plasma membrane, ER, or GC. Cytoplasmic proteins may recover as rapidly as 1–20 s. In this way, the investigator can establish conditions to obtain data sufficient for estimation of $t_{1/2}$ and mobile fraction (M_f) (see below). The investigator should not attempt to refocus a cell during an FRAP experiment because the fluorescence intensities will shift and the recovery curves will no longer be smooth. Time series that contain a shift in focal

plane should be discarded. If a protein has a high protein *D* value (i.e., ≥5 $\mu m^2/s$), the investigator may not observe a defined bleach region following the photobleach, especially for slower confocal microscopes. Rapidly diffusing FPs may appear homogeneously distributed immediately following a photobleach. The investigator must either (1) increase the image collection rate, by changing the scan speed or reducing the size of the total frame to be collected, (2) increase the bleach ROI size, (3) increase the laser power or employ a combination of these suggestions.

3. Collect at least 10–20 data sets for each fluorescent reporter and treatment for robust statistical analyses. A fraction of the data sets are usually discarded because of problems that potentially bias imaging results (i.e., incomplete recovery, the focal plane shifted, cell movement, the recovery curve fitting method fails, etc.).

Note: For exceptionally rapidly moving molecules or structures (soluble proteins and vesicles), extremely rapid image acquisition speeds may be required. Newer spinning disk microscopes with sensitive electron multiplying Charge Coupled Device (emCCD) cameras or high speed acquisition microscopes, that is, the Duoscan (Carl Zeiss, Inc., Jena, Germany) or the Nikon LiveScan Swept Field Confocal microscope (Nikon Instruments, Inc., Melville, NY) can perform photobleaching operations and image at rates of tens of fps. For slower microscopes, an alternative approach is to image the photobleach ROI alone. The caveat of the method is that the cell may shift in focus or position during the course of imaging. Imaging the whole cell enables the advantage of visualizing any movement of the cell or focal plane, permitting the researcher to reject unusable data following visual inspection.

12.2.5 Inverse FRAP protocol

Inverse FRAP or iFRAP (Altan-Bonnet et al., 2006; Nichols et al., 2001) gets its name from the way in which everything *except* the region of interest is photo-bleached. Typically, this is accomplished by drawing an ROI over all parts of the cell excluding the region to be monitored, in this case, the GC. Because the ROI drawing programs only create continuous ROIs, the ROI will be drawn like a bagel with a hole in the center connected to the area outside of the cell by a narrow path (Fig. 12.4).

The iFRAP technique has three general uses. First, it can be used to perform a pulse-chase experiment. The ability of a population of proteins to exit the GC, the rate, and the types of structures that facilitate escape can be visualized (Fig. 12.4). Similar experiments can be performed with photoactivatable proteins (Lukyanov, Chudakov, Lukyanov, & Verkhusha, 2005; Shaner et al., 2007). The iFRAP technique permits the investigator to do all dynamics experiments with the same protein. Second, iFRAP helps reveal dim structures. In standard IF, all pools of a protein are labeled by an antibody. If a protein is mostly in the ER and a small fraction is in vesicles, the bright signal can overwhelm the fluorescent signal of the vesicles. iFRAP enables the investigator to remove the ER signal and dramatically improve the signal to noise for very dim vesicles. Third, iFRAP compliments data from FRAP and FLIP experiments. While FRAP quantitates rate of recovery of fluorescence into an ROI, iFRAP can be used to measure rate of fluorescence loss from an ROI. FLIP helps visualize immobilized pools of FPs or discontinuous compartments.

Prepare sample and microscope as for FRAP. The key difference is that the photobleach ROI will be drawn to exclude the GC or other fluorescent structure of interest. Do not draw the ROI into the edge of the GC. The photobleaching laser is not always perfectly constrained to a single pixel. Include a small border around the GC (see Fig. 12.4). If visualizing dim structures is the goal of the experiment, it is often helpful to increase the image intensity (i.e., increased gain, more laser power, slower scan speed). After the photobleach, the dim structures will be often bright enough to detect against the otherwise dark background.

12.2.6 Fluorescence loss in photobleaching protocol

As in FRAP, fluorescence loss in photobleaching (FLIP) photobleaches an ROI with a high power laser. However, in FLIP, the ROI is repeatedly photobleached and the cell is alternatingly imaged to examine the behavior of the entire fluorescent pool throughout a structure or the cell. If the fluorescent molecules are completely mobile and have access to the photobleaching ROI, the entire fluorescent pool will be depleted (see Fig. 12.5). Thus, results from FLIP experiments can reveal the connectedness of structures containing FP reporters (Ellenberg et al., 1997; Nehls et al., 2000). FLIP can also be used to look at dynamics of proteins that bind and release from the GC surface, such as COP molecules (Presley et al., 2002).

In FLIP analysis, the user obtains a prebleach image, an immediate postbleach image following the first photobleach, images following successive photobleaches (often two to three images following each photobleach) until the entire cell or structure is depleted of fluorescence or several successive photobleaches do not further deplete cell fluorescence, the time for each image, pixel size, and fluorescence intensity values for the whole cell and the background intensity:

1. Prepare microscope and cells as in the FRAP protocol.
2. Identify the cell of interest on the confocal microscope. The optimal condition is to have two adjacent cells of similar fluorescence intensity in the imaging field. The unbleached cell serves as a control to insure that the imaging conditions do not cause nonspecific photobleaching of all fluorescence in the field of view. Imaging conditions must not significantly photobleach any adjacent cells during the experiment. The cell will often be imaged 100–1000 times during a FLIP experiment and that number of exposures will inherently cause photobleaching. Thus, it is important to image the cell with the fastest possible scan and lowest laser power to minimize photobleaching. Bring the desired cell into focus. Scan an image of the whole cell at the desired excitation light intensity, averaging, etc. Modify pinhole and detector gain for maximal fluorescence signal and minimal pixel saturation. Detector gain and offset will vary depending on the concentration of the fluorophore, the laser power, objective used, and the thickness of the fluorescently labeled organelle or region. The imaging parameters used for the prebleach image(s) should be used for the fluorescence recovery time series.

3. Define an ROI for the photobleach. The bleach ROI should be between 5% and 20% of the structure of interest. The photobleach ROI does not need to be a strip. A square or circle is equally appropriate.

4. Determine imaging and photobleaching conditions (i.e., scan speed, zoom, laser power, number of laser iterations required for photobleaching, microscope objective) that cause minimal photobleaching of the cell outside the photobleach ROI. For example, a 40-mW 488-/514-nm argon laser can be used at 45–60% power with 10–20% transmission for photobleaching and 1% transmission for imaging on a Zeiss 510. For a Zeiss Duoscan, a 100-mW 489-nm laser is used at 100% transmission, scan speed 9, one bleach iteration. The photobleach does not need to be as strong as in an FRAP experiment. Molecules will continuously diffuse through the ROI and should eventually be photobleached even at the lower intensity. A benefit of this approach is that the cell should be less stressed by the laser over the course of the FLIP experiment. Depending on the microscope, a field of cells (or a smaller imaging ROI if using a laser scanning confocal microscope) can be scanned at 0.1–2 s per image with two to four line or frame averaging (less averaging for series with increasing numbers of total exposures).

5. Collect 10 prebleach images to establish the prebleach fluorescence intensity and to confirm that the prebleach fluorescence intensity does not significantly fluctuate.

6. Photobleach the bleach ROI. Collect two images of the whole cell and photobleach the ROI again. Repeat the process until the fluorescent structure intensity is similar to background. Unlike FRAP, speed of imaging is not critical for most FLIP experiments. Bear in mind that the bleaches in the FLIP experiment are most useful when the bleach can further deplete fluorescence. If bleaches are performed too quickly in succession, there may be little recovery of fluorescence into the ROI and the next photobleach will have no productive effect. Typically, a delay of 1–5 s between images and the next photobleach works well. The delays allow unbleached molecules to diffuse into the photobleached ROI. Furthermore, collecting images between bleaches permits monitoring of FLIP progress and confirms that the cell remains in focus and has not moved. It is acceptable to refocus the cell during a FLIP experiment. Great care must be taken to return to the original focal plane. Shielding the stage from air currents in a room and minimizing temperature fluctuations on the stage can help maintain focus. Autofocus routines available for some microscopes can also help. Cell movement is more problematic. Extensive movement will mean the original ROI may be a significant distance away at the end of an experiment. Then the FLIP is not spatially restricted and other parts of the cell could be directly photobleached, which is counter to the goal of the FLIP experiment. If the cell moves significantly, the experimental results are unusable. For exceptionally slow proteins, the delay between images can be even longer. It is also acceptable to increase the size of the bleach ROI to decrease the time needed to deplete total structure fluorescence. It may require some experimentation to identify the best sized bleach area to maximize the number of data points for a well-defined fluorescence intensity data curve, while minimizing the time of imaging to prevent general photobleaching of the cell.

7. Collect at least 5–10 data sets for each FP reporter and treatment. Note that some data sets may be unusable due to focal plane shift, the cell movement, etc.

12.2.7 Data analyses: Quantitation of photobleaching data

After collecting photobleaching data, there are three general parameters that can be determined: the M_f of the FP reporter, its diffusion coefficient (D), and the $t_{1/2}$ of the fluorescence recovery or loss. Each parameter has potential utility. To make the most of the collected data, the investigator should perform calibration experiments with an FP reporter whose mobility properties have been previously characterized, especially when calculating D values.

12.2.7.1 Mobile fraction—M_f is the percentage of FPs capable of diffusing into a photobleached ROI during the time of the experiment. M_f, D, and $t_{1/2}$ are distinct parameters and must be understood as such. D is a characteristic of the mobile pool of FPs. The proteins in the *immobile* fraction do not diffuse or contribute to the D value. A low D value does not bear any relation to the fraction of immobile proteins.

An approximation of M_f can be calculated using the following equation, based on (Feder, Brust-Mascher, Slattery, Baird, & Webb, 1996) with the inclusion of a photo-bleaching correction (Lippincott-Schwartz, Snapp, & Kenworthy, 2001). Given the focus of this chapter, it is assumed that FRAP will be performed primarily on the GC. As diffusion will be relatively fast compared to rates of trafficking and protein synthesis, the fluorescence pool for recovery will be mostly confined to the GC:

$$M_f = 100 * \frac{(F_{PreGC} - F_{\text{background}})}{(F_{\infty GC} - F_{\text{background}}} * \frac{(F_{\infty} - F_{\text{background}})}{(F_{pre} - F_{\text{background}})}$$

where F_{preGC} is the whole GC prebleach intensity, F_{pre} is the bleach ROI prebleach intensity, $F_{\infty\text{GC}}$ is the asymptote of fluorescence recovery of the whole GC, $F_{\text{background}}$ is the mean background intensity, and $F\infty$ is the bleach ROI asymptote.

In the equation, the photobleach ROI and whole GC ROIs are background subtracted. Next, the photobleach ROI data are transformed such that the prebleach fluorescence intensity is defined as 100% fluorescence intensity. The equation includes a correction for the loss of total GC fluorescence (due to the photobleach of the ROI and bleaching of the GC during imaging). The correction is calculated by determining the prebleach fluorescence intensity of the whole GC ROI (F_{preGC}) and dividing it by the whole GC ROI intensity at time "*t*." Without the photobleach correction, the bleach ROI intensity can never recover to 100% of the prebleach fluorescence because the photobleach depletes 5–50% of the total GC fluorescence (see Fig. 12.3). To convert the fraction to a percentage, the data are multiplied by 100.

12.2.7.2 Diffusion analysis—D values reflect the mean squared displacement (usually $\mu m^2/s$ or cm^2/s, which can be multiplied by 10^8 to get $\mu m^2/s$) that a protein explores through a random walk (i.e., Brownian motion) over time. D values do NOT correspond to a linear

process. The time required to cover increasing distances does not increase in a linear fashion. Time to sample increasing distances increases as the square of the distance covered divided by the *D* value. The primary constraints on protein diffusion are the viscosity of the environment (η), whether the protein is soluble or integrated into a membrane, and to a lesser extent, the hydrodynamic radius (R_h) of the protein. Protein–protein interactions and collisions with other molecules hinder free diffusion. By measuring *D* values, the investigator can obtain information related to a protein's environment and in some cases, whether the protein is interacting with large complexes.

Several equations and computer simulations have been developed to determine *D* values (Axelrod, Koppel, Schlessinger, Elson, & Webb, 1976; Gordon, Chazotte, Wang, & Herman, 1995; Saxton, 2001). Many available equations have been written for spot photobleaching or have been developed for highly specialized scenarios (i.e., the nuclear environment or the plasma membrane). Therefore, it is important to appreciate that many diffusion analytical methods are not necessarily appropriate for studies of the GC. The author has tried simulations developed for cells, in general, as well as simulations developed by microscope companies. Control protein *D* values were often incorrect by an order of magnitude or more. The problem is that most equations and simulations make important assumptions that may not hold true in the GC. In some cases, equations do not take into account the inhomogeneous diffusion that occurs in cellular compartments. The bottom line is one must validate a diffusion analysis method with robust control proteins. Do not simply accept values produced by an equation without establishing that the values are reasonable. For example, a membrane protein should not diffuse faster than 0.8–1.0 $\mu m^2/s$.

A robust method we have found for obtaining *D* value is through simulation of diffusive recovery into a bleached strip (Siggia, Lippincott-Schwartz, & Bekiranov, 2000). The Siggia simulation models inhomogeneous diffusion of unbleached proteins in the cell into the photobleach ROI. The simulation then compares the simulated recovery to the actual data to determine *D* (Siggia et al., 2000). The program has been used for ER membrane proteins (Ellenberg et al., 1997; Zaal et al., 1999) and has been used to calculate *D*s comparable to values observed by other labs using different methods. Like other methods for determining *D*, simulation encounters difficulties when a significant fraction of the FP is immobilized (Siggia et al., 2000). In such cases, the simulation either fails to fit the simulation data to the experimental recovery data or the simulation cannot calculate *D*.

The Siggia simulation and a set of instructions can be obtained by contacting this author. The simulation has been written for UNIX systems and has been compiled for Apple computers pre-Intel chip (running OS × 10.4 and earlier). Recently, we were able to get the program successfully compiled for newer Apple computers.

After running any simulation or calculating a least squares fit to determine *D*, it is essential to compare the simulation or fit data to the experimental data by plotting the data sets in a spreadsheet program. Even if a program or equation produces *D*, a poor fit means that *D* is questionable at best. “Goodness of fit” describes how well the simulation or equation data overlaps the experimental data. The majority of the experimental data must overlap the simulation or equation plot. If the simulation misses the experimental data, the calculated *D*

is questionable, at best. If there are any doubts about "goodness of fit," the user should consider another method of calculating the *D*.

Potential errors may occur in the course of data fitting. These errors are not unique to *D* calculations. They are part of the general problem of nonlinear regression analysis. Individuals interested in performing diffusion analysis can learn more about nonlinear regression analysis in an excellent (and free!) introduction to the theory and problems of nonlinear regression analysis at http://www.graphpad.com/guides/prism/6/curve-fitting/.

12.2.7.3 $t_{1/2}$ analysis—The mobility of several proteins depends on complex behaviors, such as binding and release or populations with multiple *D*s. The architecture of a cellular structure can increase apparent *D* values by increasing the path length that a molecule must traverse (Sbalzarini, Mezzacasa, Helenius, & Koumoutsakos, 2005). Diffusion in the GC is further complicated by the extent of connectedness between cisternae (Patterson et al., 2008; Trucco et al., 2004). That is, when observing recovery, is it just from the remaining contents of a partially bleached cistern or also from a connected unbleached cistern. Such conditions complicate the analysis of *D* and may prevent fitting of data by traditional diffusion analysis.

When a diffusion equation or simulation is unable to fit fluorescence recoveries, the $t_{1/2}$ can be used to compare relative recovery rates between samples. The $t_{1/2}$ is the time in which the fluorescence intensity in the bleach ROI recovers to 50% of the asymptote or plateau fluorescence intensity. This value is independent of the pre-bleach ROI fluorescence intensity. While the $t_{1/2}$ can be a useful tool, it is only relevant for the user's system and conditions. The $t_{1/2}$ cannot be compared to $t_{1/2}$ values obtained by other investigators since the $t_{1/2}$ depends on the experimental setup.

To perform $t_{1/2}$ analysis, the data must have been collected using identical acquisition conditions—the same bleach ROI, number of bleach iterations, scan rate, frame rate, laser power, and even relative bleach ROI position (i.e., if the ROI is at the edge of the GC, all other ROIs must be similarly placed. If one ROI is on the edge and the next is in the middle, then one would receive fluorescence from one side and the other ROI would receive fluorescence from two sides, which should significantly impact the recovery rate).

The $t_{1/2}$ requires one data manipulation, conversion of the photobleach ROI recovery data into fractional fluorescence. The $t_{1/2}$ can be determined visually or by solving the following equation for each data set (Feder et al., 1996):

$$F(t) = \frac{\left[F_0 + F_\infty\left(\frac{t}{t_{1/2}}\right)\right]}{\left(1+\left(\frac{t}{t_{1/2}}\right)\right)}$$

F_0 is the bleach ROI immediate postbleach intensity

$F\infty$ is the asymptote of the bleach ROI fluorescence recovery

t is the time for each ROI intensity value, usually in seconds or milliseconds

$t_{1/2}$ is the time required for the bleach ROI to recover to 50% of the asymptote.

12.2.7.4 Calculation of fractional fluorescence—To directly visualize and determine the $t_{1/2}$, transform the fluorescence intensity ($F(t)$) data to a 0–100% scale (see Fig. 12.4). The measurement is independent of the prebleach intensity and is not bleach corrected, as the relevant data occurs after the photobleach. The fluorescence recovery into the photobleach ROI must form a genuine plateau or asymptote or $t_{1/2}$ analysis cannot be performed. It is also important to have a large signal difference between the first postbleach intensity and the plateau. If the signal difference is too small, the plotted recovery will tend to be very broad and difficult to interpret. The following equation will convert ($F_2(t)$) the bleach ROI fluorescence recovery into fractional fluorescence data:

$$F_2(t) = 100 \times \frac{[F(t) - F_0]}{[F_\infty - F_0]}$$

$F(t)$ is the bleach ROI fluorescence intensity at time t

F_0 is the immediate postbleach bleach ROI fluorescence intensity

$F\infty$ is the asymptote of the bleach ROI fluorescence recovery

The F_2(t) data are plotted versus time (in seconds) to determine $t_{1/2}$.

12.3 DISCUSSION

After acquiring and analyzing photobleaching data, one must still consider the problem of how to interpret the results. Few cellular proteins diffuse in a true random walk. Instead, diffusion barriers (i.e., the cytoskeleton, the nuclear pore, barriers within membranes, etc.), bind and release of proteins from membranes or relatively immobile proteins, and nondiffusive movements (i.e., motor proteins, vesicular traffic) all impact molecular movement relevant to the GC. Thus, standard diffusion analysis may be inappropriate for many investigations into GC function. While often noisy, $t_{1/2}$ measurements make no assumptions concerning the nature of molecular movement and can be used to make comparative measurements. Ultimately, most interesting photobleaching experiments concern comparative rather than absolute measurements. The effects of a treatment or mutant on the mobility of a protein primarily concern whether there is a change and how much change there is. Determining a D value certainly can be useful as it can be compared across a wide range of reported results, while $t_{1/2}$ values can only be directly compared for experiments with the identical microscope setup and imaging parameters.

With the availability of multiple spectrally distinct FPs, the investigator is encouraged to perform experiments with a control protein and the protein of interest in the same cell. Most confocal microscopes are equipped with multiple lasers and it should be possible to simultaneously photobleach two (or even three) different FP reporters within the same GC.

Today, the investigator is limited primarily by imagination in the study of GC proteins and membranes. Modern laser scanning confocal microscopes are sensitive enough and fast

enough to image most GC proteins. The newer FPs ensure that reporters can behave more physiologically. The greatest limitation remains resolution of molecular movements at high speeds in individual cisternae. Superresolution microscopy techniques (Hell, 2007) suggest even this may be possible.

SUMMARY

Photobleaching of FPs in living cells is a powerful technology. As described here, the choice of FPs can adversely affect experimental results. Therefore, choosing sfGFP variants, truly monomeric proteins, and maintaining a healthy skepticism of untested FPs is critical for physiologic studies of the secretory pathway. Defining the capabilities of one's microscope is also critical for successful experiments. Insufficient laser power can mean the difference between an intentional FRAP experiment and an unintentional FLIP experiment. Finally, it is important to carefully consider the choice of quantitative analyses for different types of proteins and organelle structures. With the methods and considerations described in this chapter, investigators should be well positioned to exploit photobleaching microscopy techniques.

Acknowledgments

The author is supported by a grant to the Marion Bessin Liver Center (NIH/NIDDK 5 P30 DK041296) and is grateful for the use of microscopes in the Albert Einstein College of Medicine Analytical Imaging Facility and the resources of the Cell Structure and Imaging Core of the Marion Bessin Liver Center.

References

Altan-Bonnet N, Sougrat R, Liu W, Snapp EL, Ward T, Lippincott-Schwartz J. Golgi inheritance in mammalian cells is mediated through endoplasmic reticulum export activities. Molecular Biology of the Cell. 2006; 17:990–1005. [PubMed: 16314396]

Aronson DE, Costantini LM, Snapp EL. Superfolder GFP is fluorescent in oxidizing environments when targeted via the Sec translocon. Traffic. 2011; 12:543–548. [PubMed: 21255213]

Axelrod D, Koppel DE, Schlessinger J, Elson E, Webb WW. Mobility measurement by analysis of fluorescence photobleaching recovery kinetics. Biophysical Journal. 1976; 16:1055–1069. [PubMed: 786399]

Cole NB, Smith CL, Sicaky N, Terasaki M, Edidin M, Lippincott-Schwartz J. Diffusional mobility of Golgi proteins in membranes of living cells. Science. 1996; 273:797–801. [PubMed: 8670420]

Costantini LM, Fossati M, Francolini M, Snapp EL. Assessing the tendency of fluorescent proteins to oligomerize under physiologic conditions. Traffic. 2012; 13:643–649. [PubMed: 22289035]

Costantini LM, Subach OM, Jaureguiberry-Bravo M, Verkhusha VV, Snapp EL. Cysteineless non-glycosylated monomeric blue fluorescent protein, secBFP2, for studies in the eukaryotic secretory pathway. Biochemical and Biophysical Research Communications. 2013; 430:1114–1119. [PubMed: 23257162]

Ellenberg J, Siggia ED, Moreira JE, Smith CL, Presley JF, Worman HJ, et al. Nuclear membrane dynamics and reassembly in living cells: Targeting of an inner nuclear membrane protein in interphase and mitosis. Journal of Cell Biology. 1997; 138:1193–1206. [PubMed: 9298976]

Feder TJ, Brust-Mascher I, Slattery JP, Baird B, Webb WW. Constrained diffusion or immobile fraction on cell surfaces: A new interpretation. Biophysical Journal. 1996; 70:2767–2773. [PubMed: 8744314]

Gordon GW, Chazotte B, Wang XF, Herman B. Analysis of simulated and experimental fluorescence recovery after photobleaching. Data for two diffusing components. Biophysical Journal. 1995; 68:766–778. [PubMed: 7756543]

Hell SW. Far-field optical nanoscopy. Science. 2007; 316:1153–1158. [PubMed: 17525330]

Jain RK, Joyce PB, Molinete M, Halban PA, Gorr SU. Oligomerization of green fluorescent protein in the secretory pathway of endocrine cells. Biochemical Journal. 2001; 360:645–649. [PubMed: 11736655]

Lajoie P, Snapp EL. Formation and toxicity of soluble polyglutamine oligomers in living cells. PLoS One. 2010; 5:e15245. [PubMed: 21209946]

Lippincott-Schwartz J, Snapp E, Kenworthy A. Studying protein dynamics in living cells. Nature Reviews. Molecular Cell Biology. 2001; 2:444–456.

Lukyanov KA, Chudakov DM, Lukyanov S, Verkhusha VV. Innovation: Photoactivatable fluorescent proteins. Nature Reviews. Molecular Cell Biology. 2005; 6:885–891.

Nehls S, Snapp EL, Cole NB, Zaal KJ, Kenworthy AK, Roberts TH, et al. Dynamics and retention of misfolded proteins in native ER membranes. Nature Cell Biology. 2000; 2:288–295.

Nichols BJ, Kenworthy AK, Polishchuk RS, Lodge R, Roberts TH, Hirschberg K, et al. Rapid cycling of lipid raft markers between the cell surface and Golgi complex. Journal of Cell Biology. 2001; 153:529–541. [PubMed: 11331304]

Paroutis P, Touret N, Grinstein S. The pH of the secretory pathway: Measurement, determinants, and regulation. Physiology (Bethesda). 2004; 19:207–215. [PubMed: 15304635]

Patterson GH, Hirschberg K, Polishchuk RS, Gerlich D, Phair RD, Lippincott-Schwartz J. Transport through the Golgi apparatus by rapid partitioning within a two-phase membrane system. Cell. 2008; 133:1055–1067. [PubMed: 18555781]

Pedelacq JD, Cabantous S, Tran T, Terwilliger TC, Waldo GS. Engineering and characterization of a superfolder green fluorescent protein. Nature Biotechnology. 2006; 24:79–88.

Presley JF, Ward TH, Pfeifer AC, Siggia ED, Phair RD, Lippincott-Schwartz J. Dissection of COPI and Arf1 dynamics in vivo and role in Golgi membrane transport. Nature. 2002; 417:187–193. [PubMed: 12000962]

Saxton MJ. Anomalous subdiffusion in fluorescence photobleaching recovery: A Monte Carlo study. Biophysical Journal. 2001; 81:2226–2240. [PubMed: 11566793]

Sbalzarini IF, Mezzacasa A, Helenius A, Koumoutsakos P. Effects of organ-elle shape on fluorescence recovery after photobleaching. Biophysical Journal. 2005; 89:1482–1492. [PubMed: 15951382]

Shaner NC, Patterson GH, Davidson MW. Advances in fluorescent protein technology. Journal of Cell Science. 2007; 120:4247–4260. [PubMed: 18057027]

Siggia ED, Lippincott-Schwartz J, Bekiranov S. Diffusion in inhomogeneous media: Theory and simulations applied to whole cell photobleach recovery. Biophysical Journal. 2000; 79:1761–1770. [PubMed: 11023884]

Snapp EL, Hegde RS, Francolini M, Lombardo F, Colombo S, Pedrazzini E, et al. Formation of stacked ER cisternae by low affinity protein interactions. Journal of Cell Biology. 2003; 163:257–269. [PubMed: 14581454]

Swaminathan R, Hoang CP, Verkman AS. Photobleaching recovery and anisotropy decay of green fluorescent protein GFP-S65T in solution and cells: Cytoplasmic viscosity probed by green fluorescent protein translational and rotational diffusion. Biophysical Journal. 1997; 72:1900–1907. [PubMed: 9083693]

Trucco A, Polishchuk RS, Martella O, Di Pentima A, Fusella A, Di Giandomenico D, et al. Secretory traffic triggers the formation of tubular continuities across Golgi sub-compartments. Nature Cell Biology. 2004; 6:1071–1081.

Zaal KJ, Smith CL, Polishchuk RS, Altan N, Cole NB, Ellenberg J, et al. Golgi membranes are absorbed into and reemerge from the ER during mitosis. Cell. 1999; 99:589–601. [PubMed: 10612395]

Zacharias DA, Violin JD, Newton AC, Tsien RY. Partitioning of lipid-modified monomeric GFPs into membrane microdomains of live cells. Science. 2002; 296:913–916. [PubMed: 11988576]

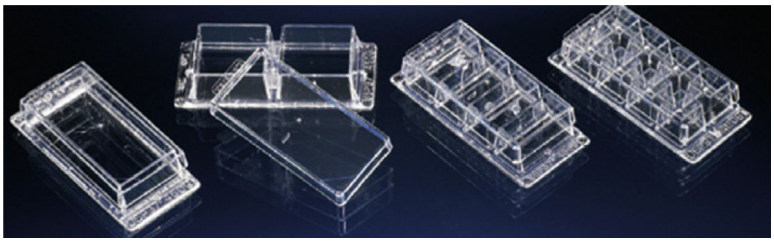

FIGURE 12.1.
Lab-Tek chambered coverglasses.

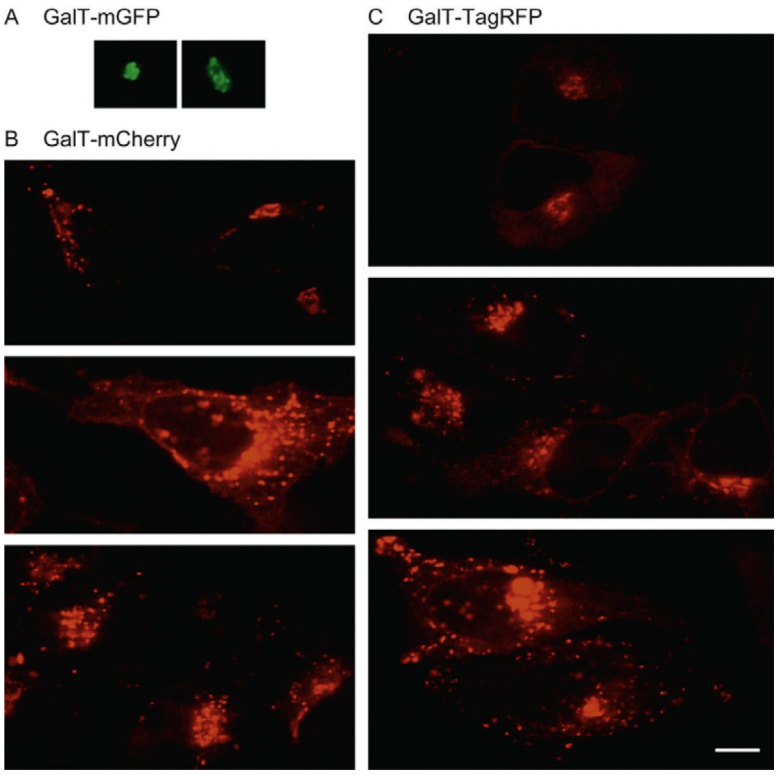

FIGURE 12.2.

Effects of FP on GC structure. Fluorescence images of HeLa cells expressing GalT-mGFP (A), GalT-mCherry (B), and GalT (TagRFP) (C). In the lowest expressing cells in (B) and (C) (top panels), compact GC structures comparable to GalT-mGFP structures are observed. In modest to high expressing cells, the red constructs label dispersed punctate structures throughout the cell. For this reason, current red FPs are generally not suitable for secretory pathway membrane protein fusions. Scale bar is for all images and is equal to 10 μm.

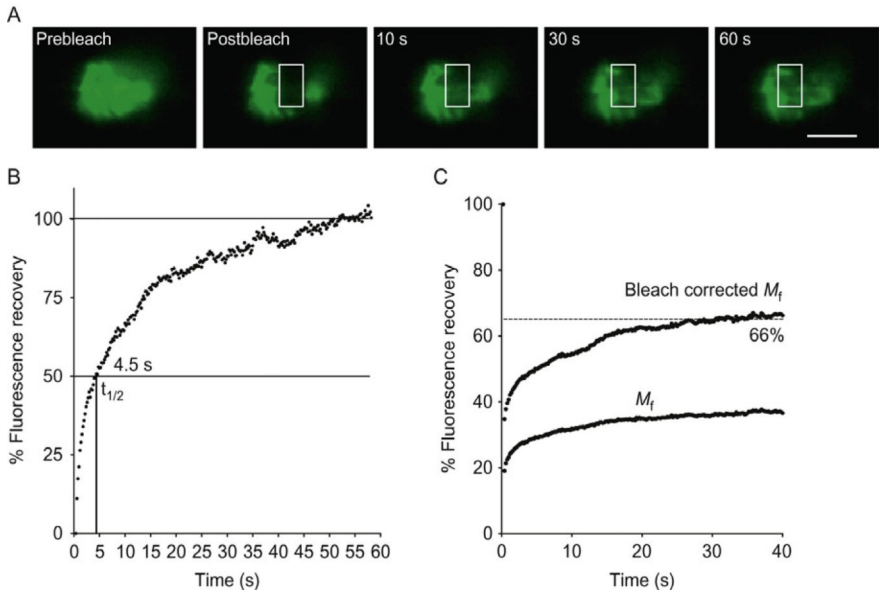

FIGURE 12.3.

Golgi complex FRAP. (A) FRAP of a GC in HeLa cell expressing secretory sfGFP. (B) Plot of recovery data transformed for $t_{1/2}$ analysis. Note that prebleach intensity is not relevant to $t_{1/2}$ analysis. (C) Plots of M_f and bleach-corrected M_f data. The bleach-corrected M_f accounts for the substantial loss of total GC fluorescence and reveals a substantially higher value than the uncorrected M_f.

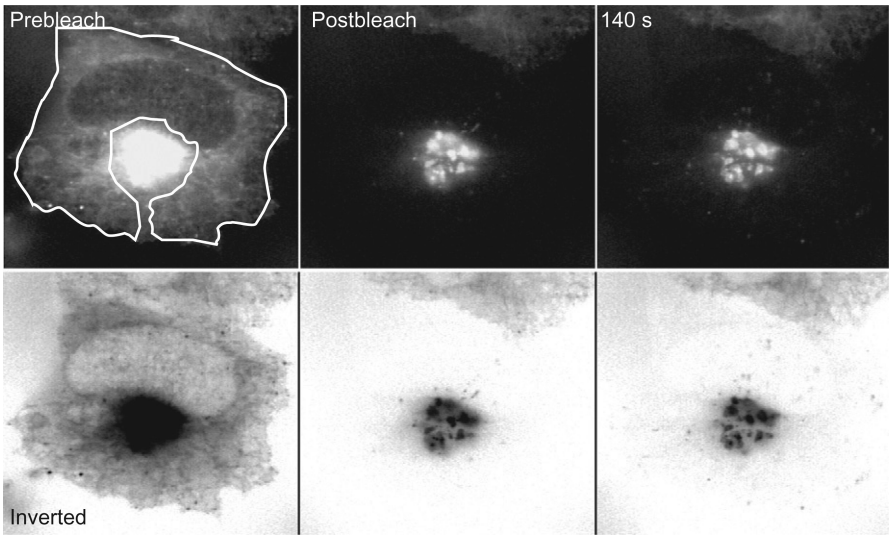

FIGURE 12.4.

iFRAP of HeLa cell expressing VSV G-sfGFP. A “bagel bleach” ROI was drawn over the entire cell and excluded the GC. Immediately after the photobleach and especially after 140 s, dim vesicles and tubules can be visualized emerging from the GC. The image series also has been inverted to help visualize the number and variety of vesicles.

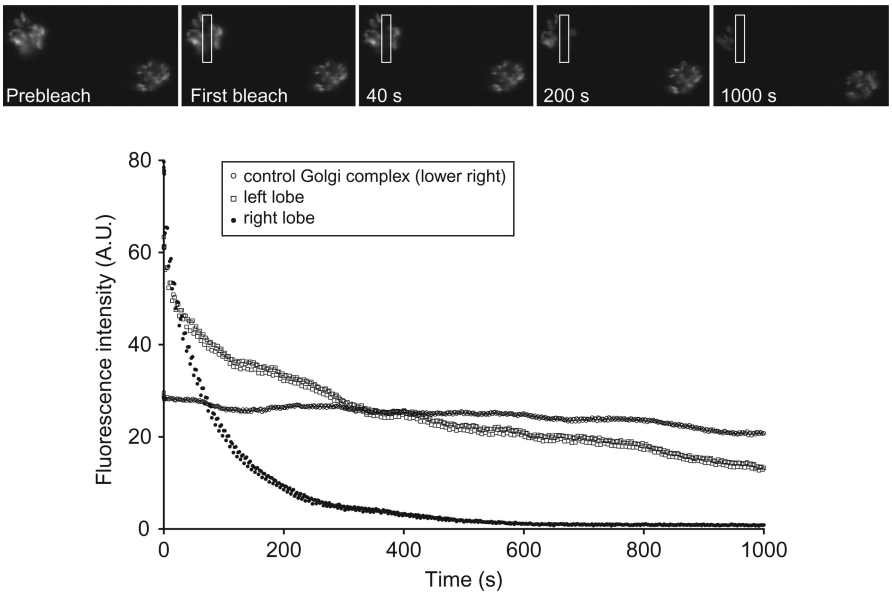

FIGURE 12.5.

FLIP of GalT-GFP in HeLa cell. A bleach region of interest (ROI) was placed in the middle of the GC and bleached after every three images, collected with 2 s delay between images. The plot shows the different rates of loss of fluorescence for the two sides (lobes) of the GC, as well as the control GC in the lower right corner. Note that the control GC loses very little fluorescence, indicating that fluorescence loss in the GC of interest is specifically due to bleaching of the ROI. The two lobes lose fluorescence at different rates, suggesting that the reporter construct is either organized differently within domains of the GC and/or that there may be different rates of communication within this GC structure, that is, discontinuous cisternae.